A proton current drives action potentials in genetically identified sour taste cells

Rui B. Chang, Hang Waters, and Emily R. Liman[1]

Department of Biological Sciences, Section of Neurobiology, University of Southern California, Los Angeles, CA 90089

Edited* by King-Wai Yau, The Johns Hopkins School of Medicine, Baltimore, MD, and approved October 29, 2010 (received for review September 16, 2010)

Five tastes have been identified, each of which is transduced by a separate set of taste cells. Of these sour, which is associated with acid stimuli, is the least understood. Genetic ablation experiments have established that sour is detected by a subset of taste cells that express the TRP channel PKD2L1 and its partner PKD1L3, however the mechanisms by which this subset of cells detects acids remain unclear. Previous efforts to understand sour taste transduction have been hindered because sour responsive cells represent only a small fraction of cells in a taste bud, and numerous ion channels with no role in sour sensing are sensitive to acidic pH. To identify acid-sensitive conductances unique to sour cells, we created genetically modified mice in which sour cells were marked by expression of YFP under the control of the PKD2L1 promoter. To measure responses to sour stimuli we developed a method in which suction electrode recording is combined with UV photolysis of NPE-caged proton. Using these methods, we report that responses to sour stimuli are not mediated by Na^+ permeable channels as previously thought, but instead are mediated by a proton conductance specific to PKD2L1-expressing taste cells. This conductance is sufficient to drive action potential firing in response to acid stimuli, is enriched in the apical membrane of PKD2L1-expressing taste cells and is not affected by targeted deletion of the PKD1L3 gene. We conclude that, during sour transduction, protons enter through an apical proton conductance to directly depolarize the taste cell membrane.

gustatory | mouse | TRPM5 | acetic acid | HCl

Most vertebrate species are responsive to five basic tastes: sweet, bitter, umami, sour, and salty, each of which provides distinct information on the nutritional content and safety of ingested food and is detected by a separate subset of cells within the taste bud (1). Although great strides have been made in understanding the sensory transduction cascade involved in bitter, sweet, and umami taste, and more recently in salty taste (2), relatively little is known about sour. Recent studies using genetic ablation have clearly demonstrated that sour taste is detected by a subset of taste cells defined by expression of the TRP ion channel PKD2L1 (3). However, the ionic mechanisms that underlie sensory responses to sour remain poorly understood.

Substances that taste sour are acidic and include fermented foods and unripe fruits. Psychophysical studies in humans have shown that sour is elicited by solutions containing HCl at concentrations >1 mM (pH 3) (4), suggesting that an acidic extracellular pH is a stimulus for sour. In addition, it has been proposed that intracellular acidification contributes to sour taste (5, 6), as weak acids that induce intracellular acidification, such as acetic acid, produce a more intense sour sensation than do strong acids (4). Consistent with a role for extracellular protons in sour sensing, it was recently shown that sour responses elicited by CO_2 are dependent not on intracellular conversion of CO_2 to bicarbonate (which releases a proton), but rather on extracellular conversion of CO_2 to bicarbonate (7). Several candidate molecules have been proposed to mediate detection of sour, including acid-sensing ion channels (ASICs), hyperpolarization activated channels (HCNs), two-pore domain K^+ channels, and most recently the PKD2L1/PKD1L3 heterodimer, a member of the transient receptor channel family (8–15). However, direct evidence linking any of these receptors to sour taste is still lacking (16). Notably, although an initial report showed that the PKD2L1/PKD1L3 heteromer was activated by exposure to solutions of low pH (pH <3) (14), subsequent reports show that activation occurs at a delay upon removal of the acid (17, 18). Moreover, a recent study of mice carrying a targeted deletion of PKD1L3 found no significant deficits in behavioral or nerve responses to sour stimuli (19).

The study of sour taste has been problematic for two reasons: First, the taste bud is heterogeneous and only ~20% are expected to be sour responsive (3, 13, 14); and second, many ion channels with no role in sour sensing are either blocked or activated by acidic pH (20). Thus, at present no study has documented the presence of a proton-sensitive conductance that is specific to sour-responsive taste cells and is therefore a candidate to mediate sour transduction. To identify such a conductance, we generated mice in which yellow fluorescent protein (YFP) is driven by the promoter of PKD2L1. To identify responses specific to this subset of cells, we also measured responses from cells that express GFP driven by the promoter of TRPM5, a downstream element of the signal transduction cascade, and a marker for cells responsive to bitter, sweet, and umami tastes (21–23). By comparing responses from YFP-labeled cells to responses from GFP-labeled cells, we have identified a proton conductance that is specific to sour-responsive taste cells. Using a unique method of UV-uncaging of protons at the apical surface of the taste cell, combined with suction electrode recording, we demonstrate that proton entry through this conductance is sufficient to initiate the firing of action potentials in response to extracellular acidification.

Results

Functional Responses to Sour of Genetically Labeled Sour Taste Receptor Cells. PKD2L1 is expressed in a small subset of taste receptor cells that are required for nerve responses to sour stimuli (3). Using BAC modification (24) similar to that previously used to target PKD2L1 cells for genetic ablation (3), we generated mice in which the promoter of PKD2L1 drives expression of YFP (Fig. S1*A*). To compare functional properties of PKD2L1-expressing cells with those of TRPM5-expressing cells, we used a line of mice in which the TRPM5 promoter drives the expression of GFP (22, 23).

To determine whether YFP faithfully identifies the population of PKD2L1-expressing cells, we stained sections of tongue containing circumvallate papillae (Fig. 1 *A* and *B*) with a polyclonal antibody directed against mPKD2L1. We observed faithful coexpression of YFP with PKD2L1, and complete exclusion of YFP from taste receptor cells that express TRPM5. YFP could also be detected with epifluorescence in dissociated taste receptor cells from circumvallate, follate, and fungiform papillae (Fig. 1*C*). Single-cell RT-PCR of singly dissociated taste cells showed that YFP-positive taste receptor cells expressed PKD2L1 as well as

Author contributions: R.B.C., H.W. and E.R.L. designed research; R.B.C, H.W., and E.R.L. performed research; R.B.C., H.W., and E.R.L. analyzed data; and R.B.C. and E.R.L. wrote the paper.

The authors declare no conflict of interest.

*This Direct Submission article had a prearranged editor.

See Commentary on page 21955.

[1]To whom correspondence should be addressed. E-mail: liman@USC.edu.

This article contains supporting information online at www.pnas.org/lookup/suppl/doi:10.1073/pnas.1013664107/-/DCSupplemental.

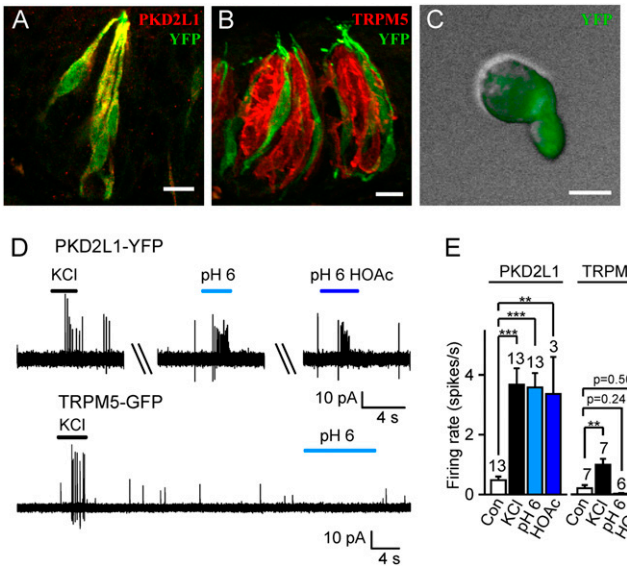

Fig. 1. YFP expression driven by the PKD2L1 promoter faithfully marks sour-responsive taste receptor cells. (*A* and *B*) In circumvallate papillae, YFP (green) is expressed by taste cells that are immunoreactive for PKD2L1 (red, *A*), but not by cells immunoreactive for TRPM5 (red, *B*). (*C*) Acutely dissociated taste cells from PKD2L1-YFP mice showed intense YFP fluorescence. (*D*) Action potentials recorded from a PKD2L1-YFP cell (*Upper*) and a TRPM5-GFP cell (*Lower*). Solutions at pH 6 were buffered with either 10 mM Mes or 10 mM acetic acid (HOAc). (*E*) Average data from experiments as in *D*. Control (con) was measured in the 10-s interval before KCl (25-mM) stimulation. Data represent mean ± SEM; $^{**}P < 0.01$; $^{***}P < 0.001$. (Scale bars: *A* and *B*, 10 μm; C, 5 μm.)

SNAP-25, as expected for this subset of cells (22, 25) but not TRPM5 (Fig. S1*B*). Moreover, patch clamp recording confirmed that PKD2L1-YFP cells have the functional properties expected for this subset of cells, including expression of voltage-gated Ca^{2+} channels (25, 26) (Fig. S2). These results clearly demonstrate that YFP expression can be used to identify PKD2L1-expressing taste cells in this BAC transgenic mouse line.

Acid-evoked action potentials (APs) have previously been detected in a subpopulation of taste cells that express GAD67 (27), which identifies the same population of cells as does PKD2L1 (25). To determine whether YFP-positive cells from PKD2L1-YFP mice respond to sour stimuli, we examined the responses of dissociated cells to acids using loose patch recordings. A 25-mM quantity of KCl, which is expected to depolarize the cell to ~ −40 mV, was used to select for cells capable of firing action potentials, and to exclude unresponsive cells from our analysis. Remarkably, all YFP cells from the PKD2L1-YFP mice that responded to KCl (13/30 cells) also responded to HCl (pH 6; 13/13 cells) and, where tested, responded to acetic acid (10 mM, pH 6; 3/3 cells; Fig. 1 *D* and *E*). Each acid stimulus evoked a burst of ~6 APs within the first 2 s. In some cells, the responses to acids could be repeated more than five times with little or no desensitization. In contrast, KCl-responsive GFP-positive cells from TRPM5-GFP mice did not respond to HCl or acetic acid ($n = 6$ and $n = 4$; Fig. 1*E*).

Together these results demonstrate that in our PKD2L1-YFP mouse line, YFP faithfully identifies PKD2L1-expressing cells. Moreover, the results show that PKD2L1-expressing cells are specifically responsive to extracellular acidification.

An Inward Current Is Specifically Activated in PKD2L1-Expressing Cells by Low Extracellular pH. To understand the ionic basis for the generation of action potentials in response to acids by PKD2L1-expressing taste cells, we measured currents evoked in response to acetic acid and HCl in whole-cell patch-clamp recording. Both pH 5 acetic acid (2 mM) and pH 5 HCl [buffered with 2-(N-morpholino) ethanesulfonic acid (Mes)] reversibly elicited inward currents in PKD2L1-expressing cells, and the average magnitude of the currents elicited by the two stimuli were no different (150.1 ± 24.2 pA versus 113.7 ± 18.0 pA at −80 mV; $n = 7$; $P = 0.28$; Fig. 2*A*). Moreover the total current measured in the presence of either stimulus, consisting of a linear inward component and a rectifying outward component, reversed at a similar voltage (26.7 ± 2.1 mV versus 28.2 ± 3.7 mV; $n = 6$–10; Fig. 2 *B* and *C*); because Mes cannot produce intracellular acidification, these data argue that, under our conditions, intracellular acidification does not contribute to the activation of an inward current. To determine whether a component of current was lost as a result of the enzymatic treatment of the cells, we measured responses under the same conditions from non-enzymatically dissociated taste cells. No differences in the magnitude or other characteristics of the current were observed (Fig. 2*C*). In the previous experiments, we used a Cs^+-based intracellular solution to reduce contributions from pH-sensitive K^+ currents (28, 29). We also measured responses from PKD2L1-expressing cells to acids with K^+ in the pipette. The magnitude of the inward current elicited by acetic acid or HCl, pH 5 (81.1 ± 28.5 pA, $n = 4$ and 176.5 ± 46.9, $n = 3$, respectively) was no different with K^+ in the pipette as compared with Cs^+ ($P = 0.11$ and $P = 0.19$, respectively). In TRPM5-expressing cells, pH 5 HCl evoked only a small inward current of 11.5 ± 6.0 pA at −80 mV (Fig. 2*C*), indicating that the acid-evoked inward current is specific to PKD2L1-expressing cells.

PKD2L1 forms a complex with PKD1L3 when expressed in HEK293 cells, and this complex has been proposed to form a sour receptor (14). To determine whether the acid-induced current we observed in sour cells is conducted by the PKD2L1/PKD1L3 channel, we crossed our BAC transgenic mice with PKD1L3 KO mice (19) and measured responses to acids from YFP positive, $PKD1L3^{-/-}$ taste cells. Notably, neither the am-

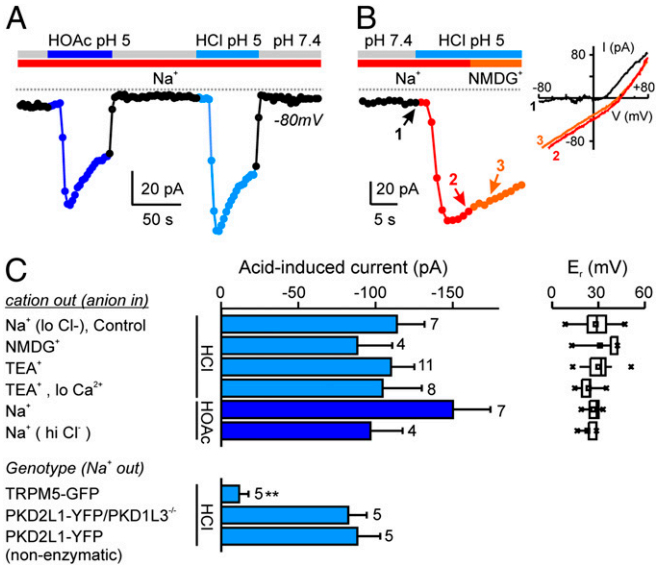

Fig. 2. Extracellular acidification specifically evokes an inward current in PKD2L1-YFP cells. (*A*) Whole-cell current at −80 mV from a PKD2L1-YFP taste cell in response to HCl pH 5 (10 mM Mes) or HOAc, pH 5 (2 mM) in the presence of extracellular Na^+. (*B*) Replacement of extracellular Na^+ with $NMDG^+$ did not affect the inward current at −80 mV in response to pH 5 (HCl). I-V relationship measured at the time points indicated are shown at *Right*. (*C*) Average magnitude of the acid-induced current at −80 mV from experiments as in *A* and *B*. Average reversal potential (Er) of the total current under each condition is shown at *Right* (n = 3–15). Note that the response is indistinguishable between HCl (Mes) and HOAc, and manipulations of the major ions (Na^+, Ca^{2+}, and Cl^-) had no effect ($P > 0.17$ for all comparisons of current magnitude with control and $P > 0.14$ for all comparisons of Er with control). Data represent the mean ± SEM. $^{**}P < 0.01$.

plitude nor the time course of the current evoked was significantly different between PKD1L3$^{-/-}$ and WT cells (Fig. 2*C*). Moreover, heterologously expressed PKD2L1/PKD1L3 did not generate an acid-activated current under the same conditions used for recording responses from taste cells (Fig. S3). Thus the acid-induced current that we recorded from sour cells is not mediated by the PKD1L3/PKD2L1 complex. Together these data establish that an acid-evoked inward current, sensitive to extracellular pH, is specifically expressed by sour-responsive taste cells.

Inward Current Activated by Acid in PKD2L1-Expressing Cells Is Carried by Protons. Many types of ion channels have been proposed to mediate sour taste transduction. To understand which, if any, of these contribute to the inward current evoked by extracellular protons in sour cells, we examined the ionic selectivity of the evoked current. Surprisingly, when we replaced Na^+ in the external solution with either of the two large cations, *N*-methyl-D-glutamine ($NMDG^+$) or tetraethylammonium (TEA^+), both of which are impermeable through nearly all known cation channels, neither the amplitude (measured at −80 mV) nor the reversal potential of the acid-induced inward current was significantly altered (Fig. 2 *B* and *C*). Moreover, lowering the concentration of external Ca^{2+} from 2 mM to 40 μM, where TEA^+ was the only other external cation, had no effect on the amplitude of the inward current or reversal potential. Thus the inward current is not carried by either of the major cations, Na^+ or Ca^{2+}. An inward current at −80 mV could also be mediated by Cl^- efflux. To test this possibility, we increased the concentration of Cl^- in the pipette from 20 mM to 150 mM, which should increase the efflux and hence the magnitude of the inward current if carried by Cl^-; again, the amplitude and reversal potential of the inward current activated by acid was unchanged (Fig. 2*C*). As this rules out possible contributions from external Na^+ and Ca^{2+} and from intracellular Cl^-, the only remaining possible charge carrier is H^+.

To determine whether the acid-induced inward current was carried by protons, we measured the effect of changing the external pH. Responses were first evident at pH 6, which corresponds to a proton concentration of 1 μM, and the amplitude of the response increased as the extracellular proton concentration increased (Fig. 3 *A* and *B*). To examine whether the current can be attributed to proton entry, we measured the reversal potential of the current at varying pH. We observed a large shift in the reversal potential (Er) of the current toward positive values as the proton concentration increased (51 mV/pH; Fig. 3 *A* and *C*), consistent with a contribution of a proton-permeable conductance to the acid-evoked current. It should be noted that we could not subtract background currents without making assumptions about their pH sensitivity. The observation that the reversal potential of the total current was consistently less than that predicted from the Nernst equation for a purely proton-selective conductance is consistent with contributions from either cationic or anionic conductances.

To further characterize the proton current in PKD2L1-expressing cells, we examined the effect of a number of pharmacological agents known to block proton conductances. Proton currents through amiloride-sensitive ion channels have been proposed to play a role in sour taste transduction (30); however, amiloride did not block the proton current in PKD2L1-YFP cells (Fig. 3*D*). In addition, the following agents that affect various proton pathways did not affect the acid-activated inward current: 1 mM Cd^{2+} (an inhibitor of proton currents); 100 μM desipramine (an inhibitor of a proton permeable serotonin transporter); and 200 nM Bafilomycin A1 (an inhibitor of the proton-permeable c subunit of V-ATPase) (31) (Fig. 3*D*). Only zinc, which blocks the recently identified proton channel Hv1 as well as many other channels (31–33), produced a significant block of the current. At 1 mM, zinc produced near-complete block of the acid-evoked inward current (Fig. 3*D*), whereas at a lower concentration (100 μM) the block was incomplete (20%, $n = 2$).

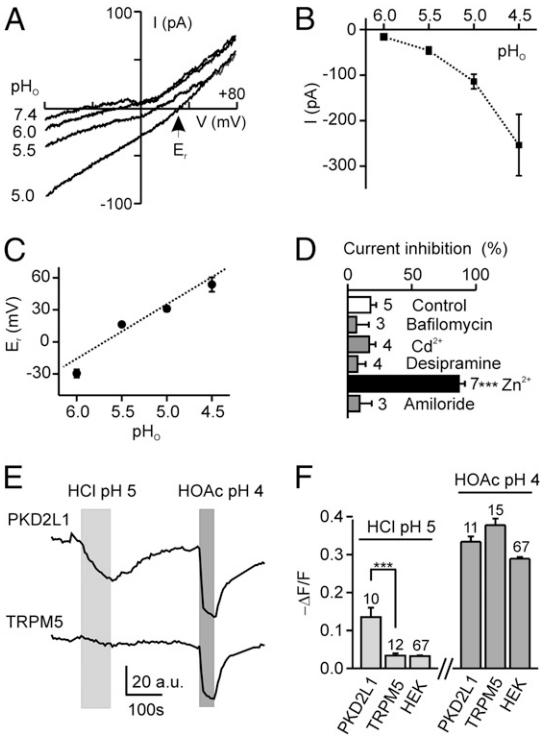

Fig. 3. The acid-evoked inward current in PKD2L1-YFP cells is conducted by protons. (*A*) Current–voltage relationship from a PKD2L1-YFP cell in response to pH 6, 5.5, and 5 (HCl) solutions under Na^+-free conditions. (*B* and *C*) Average magnitude (at −80 mV) and reversal potential of the currents from experiments as in *A* (n = 3–15). Dashed line shows a linear fit of the data with a slope of 51.0 ± 3.8 mV/pH. (*D*) Effect of indicated chemicals on current evoked by pH 5 (HCl) at −80 mV. Concentrations were as follows: 1 mM $CdCl_2$; 100 μM desipramine; 200 nM Bafilomycin A1; 1 mM $ZnCl_2$; and 30 μM amiloride. Block was measured as magnitude of current after incubation with test chemical for 10 s, as compared with magnitude of current immediately before application. No chemicals were given in the control group, and the ∼10% block represents normal rundown of current in 10 s. (*E*) Change in intracellular pH, as indicated by fluorescence intensity of carboxy-DFFDA, in response to pH 5 (HCl) and pH 4 (20 mM HOAc) solutions in a PKD2L1-YFP (*Upper*) and a TRPM5-GFP (*Lower*) taste cell. (*F*) Average data from experiments as in *E*. Data represent mean ± SEM. ***$P < 0.001$.

To confirm that proton entry occurs specifically in PKD2L1-expressing cells, we performed experiments in which the intracellular pH was monitored by a fluorescent pH indicator, carboxy-DFFDA (Fig. 3 *E* and *F*). As expected, extracellular protons were not able to cross the cell membrane in the absence of a specific transport mechanism, as no intracellular acidification was observed in response to HCl pH 5 in HEK293 cells or TRPM5-GFP taste cells. In contrast, the same acid solution caused significant intracellular acidification in PKD2L1-YFP cells (Fig. 3 *E* and *F*), consistent with the idea that a proton entry pathway exists specifically in these cells. All cells were acidified by acetic acid, which in its undissociated form can permeate the cell membrane.

Proton Entry Can Drive Action Potential Generation in PKD2L1-YFP Taste Receptor Cells. The preceding data show that we have identified a proton current that is specifically expressed by PKD2L1-expressing taste cells and that is therefore a candidate to mediate sour transduction. However, because strong acids are not readily permeable through the tight junctions of the lingual epithelium (34), to participate in transduction this proton current must be located on, although not necessarily restricted to, the apical surface of the cell. We also expect that if this current contributes to transduction, apical entry of protons should be sufficient to drive

firing of action potentials and to produce an elevation of intracellular Ca^{2+}. To address these points, we developed a method for rapidly elevating proton concentrations within a restricted cellular domain, based on UV uncaging of an NPE-caged proton (Fig. 4*A*). We further used the suction electrode recording method, which has been useful in elucidating mechanism of visual and olfactory transduction (35, 36). With this method, ionic currents can be measured from the portion of the cell that has been drawn into the pipette, and the capacitive currents produced by action potentials can be simultaneously detected, regardless of their location. In control experiments, we found that when loaded into the pipette, NPE-caged proton could, upon photolysis, activate TRPV1 channels and ASIC channels in cell-attached recording (Fig. 4*B*).

We first examined responses of taste cells when the apical region of PKD2L1-YFP cells was drawn into the pipette (Fig. 4*A*) and protons were uncaged in the pipette. A large receptor current was observed under these conditions, which was accompanied by a burst of action potentials (Fig. 4*C*; action potentials were observed in seven of eight cells). The response was specific to PKD2L1-expressing cells, as UV uncaging of protons produced only a small receptor current and no action potentials in TRPM5-expressing cells under identical conditions (Fig. 4*C*). The receptor current and accompanying action potentials in PKD2L1-expressing cells were completely blocked by 10 mM Hepes in the pipette, confirming that they were elicited in response to the changes in concentration of extracellular protons (Fig. 4*C*). As expected if protons carry the transduction current, there was no difference in the magnitude of the current or the rate of action potentials when $NMDG^+$ replaced Na^+ in the pipette solution, and the responses were completely abolished in the presence of proton-channel blocker Zn^{2+} (1 mM) (Fig. 4*C*).

To determine whether proton channels were enriched on the apical surface of the taste cells, we measured responses from the basolateral surface of PKD2L1-expressing cells. The acid-evoked current recorded from the basolateral surface was significantly smaller than the current recorded from the apical surface, and fewer action potential were evoked in this configuration (Fig. 4*C*), consistent with an enrichment of the proton current on the apical surface; however, we cannot rule out the possibility that differences in responses may be partly attributable to differences in the amount of membrane drawn into the suction electrode.

Finally, we tested a series of chemicals for their ability to block the acid-evoked current and acid-evoked action potentials. No significant effect was observed of the anion transporter blocker DIDS (200 μM), the ENaC blocker amiloride (100 μM), V-ATPase blocker DCCD (200 μM), or the Cl^- channel blocker NPPB (100 μM), although responses were somewhat smaller in the presence of the latter two blockers (Fig. S4).

Ca^{2+} imaging has been used extensively to characterize responses of taste cells to sensory stimuli, including sour substances (6, 37). To determine whether the receptor current measured in PKD2L1-expressing cells in response to uncaging of NPE-caged protons is accompanied by an elevation of intracellular Ca^{2+}, we performed simultaneous Ca^{2+} microfluorimetry. A clear elevation of intracellular Ca^{2+} was observed in response to UV uncaging of NPE-caged protons on the apical surface of the cells (Fig. 5 *A* and *B*). In addition, we noted that the Ca^{2+} elevation was highest in the two cells that generated action potentials, even though these cells did not have the largest integrated receptor current (Fig. 5*B*). This result is consistent with the notion that Ca^{2+} does not contribute to the receptor current and instead the Ca^{2+} elevation is generated by voltage-gated Ca^{2+} channels (25, 26).

Discussion

Our results provide evidence that the sensor for strong acids in sour taste cells is an apical proton conductance that is specific to PKD2L1-expressing taste cells. Previous experiments have also found evidence for proton influx during sour transduction. For example, receptor potentials in frog fungiform taste cells in response to acetic acid were partially blocked by the proton pump blocker DCCD (38), and responses in hamster taste buds to citric acid under Na^+-free conditions were attributed to proton influx through amiloride-sensitive ENaCs (30). Other evidence for proton influx into taste cells comes from studies showing changes in intracellular pH in the intact taste bud in response to HCl, although sour-responsive cells were not distinguished from other types of taste cells in these studies (37, 39). In the present report, we show that a Zn^{2+}-sensitive H^+ conductance is selectively expressed in genetically identified sour taste cells, and we demonstrate the necessity of this current for sensing of strong acids by these cells. The molecular identity of the channel or transporter that underlies this current is presently unknown, as the proton conductance that we identified does not show the rectification properties expected of the recently identified voltage-gated proton channel, Hv1 (32, 33).

A number of mechanisms have previously been proposed to contribute to sour sensation, including activation of Na^+-permeable channels or block of K^+ channels by intracellular or extracellular protons. A similarly diverse set of candidate receptor molecules have been identified that include acid-sensing ion channels, hyperpolarization activated channels, two-pore

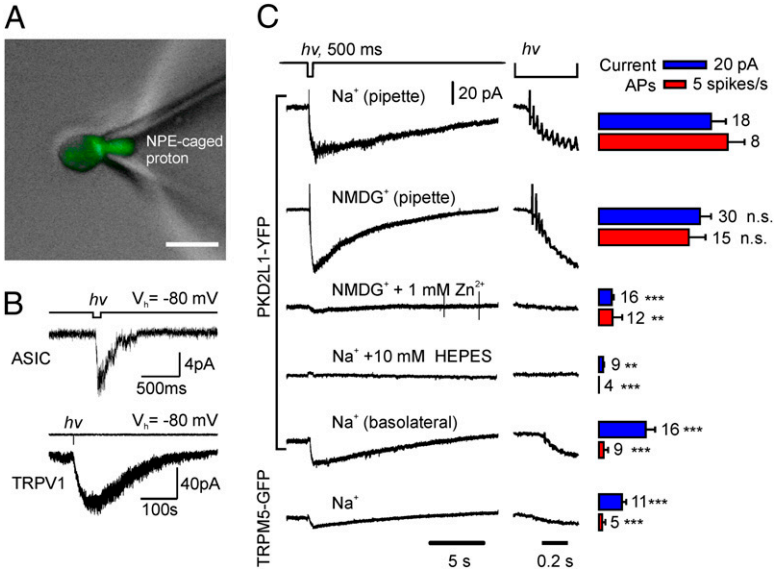

Fig. 4. Uncaging protons at the apical surface of PKD2L1-YFP cells evokes a receptor current and action potentials. (*A*) Apical membrane of a PKD2L1-YFP taste receptor cell was drawn into a suction pipette containing 2 mM NPE-caged proton. (Scale bar, 10 μm.) In this mode, the cell membrane is intact and acid stimuli can be selectively delivered to the apical surface. (*B*) Control experiments showing that UV uncaging of NPE-caged proton in patch pipette in cell-attached mode evoked endogenous ASIC currents in untransfected HEK 293 cells (*Upper*) and TRPV1 currents in HEK 293 cells transfected with TRPV1 (*Lower*). (*C*) Membrane current and action potentials recorded from taste cells upon UV uncaging of NPE-caged proton in pipette as in *A*. PKD2L1-YFP, but not TRPM5-GFP, cells responded to apical delivery of protons with a large inward current and the generation of a train of action potentials. Other traces show effects of changing the composition of the pipette solution or of recording from the basolateral surface. Average data are shown at *Right*. Blue bars represent magnitude of currents evoked by the UV flash; red bars represent the rate of evoked action potentials. Data represent mean ± SEM. $^{**}P < 0.01$, $^{***}P < 0.001$, as compared with responses from apical surface with Na^+ in pipette except for Zn^{2+}, for which the control was with $NMDG^+$ in the pipette. Responses with $NMDG^+$ in the pipette were not significantly different (n.s.) from responses with Na^+ in the pipette ($P = 0.64$ and $P = 0.13$ for current and rate of APs, respectively).

domain K^+ channels and transient receptor potential channels (9, 10, 13–15, 28–30). We have found no evidence for a contribution to sour taste of proton-gated Na^+-permeable channels such as ASIC or HCN channels, as extracellular protons did not activate an Na^+-permeable conductance in PKD2L1-expressing cells, and apical delivery of protons elicited action potentials in the absence of Na^+ ions in the apical solution. Moreover, the ENAC channel blocker amiloride had no effect on the response of sour taste cells to bath or apically applied acids. Weak acids, such as acetic acid, have been proposed to elicit sour responses by acidifying the cell cytosol, blocking potassium channels, and thereby causing membrane depolarization (5, 6, 28, 29). Our experiments, performed mostly in the absence of intracellular K^+ and under conditions that would cause only mild intracellular acidification, do not address whether this mechanism contributes to sour transduction.

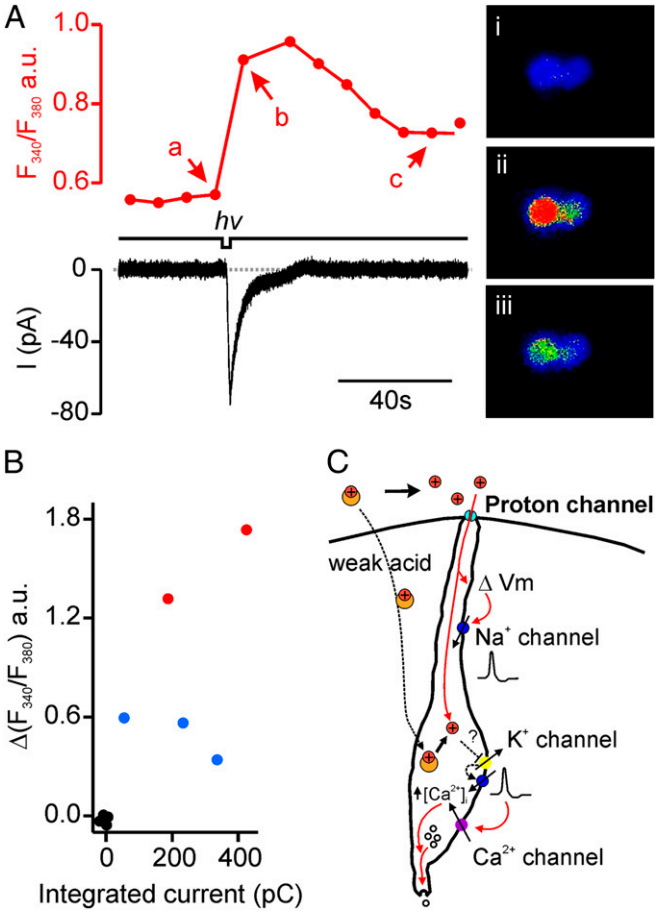

Fig. 5. Elevation of intracellular Ca^{2+} in response to apical delivery of protons in PKD2L1-YFP cells. (*A*) Simultaneous measurement of the change in intracellular Ca^{2+} (*Upper Left*) and the magnitude of current (*Lower Left*) in response to apical uncaging of NPE-caged proton in a PKD2L1-YFP cell. Fluorescent images taken at different time points are shown at *Right*. (*B*) Scatter plot of the change in intracellular Ca^{2+} as a function of the integrated current in response to UV uncaging from experiments as in *A*. Red, cells that fired action potentials; blue, cells that did not fire action potentials; black, control data measured 10 s before the UV flash. (*C*) Proposed model for sour taste transduction in PKD2L1-expressing cells. Proton entry through a proton-selective conductance specifically expressed on apical surface of PKD2L1-expressing cells leads to depolarization and generation of action potentials that propagate to the cell body and activate voltage-gated Ca^{2+} channels. In addition to accessing this pathway, weak acids may produce intracellular acidification and inhibit resting K^+ conductances.

More recently, the TRP-channel related proteins PKD1L3/PKD2L1 were identified in a subset of cells that mediate sour taste, suggesting a role in sour transduction (3, 13, 14). Although an initial report showed that the two subunits together formed a Ca^{2+}-permeable channel activated by severely acidic conditions (pH <3), later experiments showed that activation of the current occurred at a delay following washout of the stimulus (17, 18). The contribution of PKD1L3 to sour is further called into question by the observation that mice carrying a targeted deletion of PKD1L3 have normal nerve and behavioral responses to sour stimuli (19). Our results from PKD1L3 KO animals show that PKD1L3 does not directly contribute to the proton current that we have described in PKD2L1-expressing cells (Fig. 2*C*). Because PKD2L1 requires assembly with PKD1L3 to traffic normally (14, 40), these results also suggest that PKD2L1 does not contribute to the proton conductance. This conclusion is supported by our observation that the PKD1L3/PKD2L1 heteromer expressed in HEK cells did not respond to acid stimuli used to evoke proton currents in taste cells (Fig. S3). It is still possible that stronger acidification as used by Ishimaru et al. and Inada et al. (14, 17), could regulate the gating of these channels,

An important question is whether the current carried by proton entry is itself sufficient to drive the generation of action potentials. We measured an inward current of 15.82 ± 2.03 pA at −80 mV in response to a drop in extracellular to pH 6, a stimulus that was sufficient to evoke action potentials in cell-attached recording. With a measured membrane resistance of 3–5 GΩ, this would generate a membrane depolarization of >45mV, more than enough to activate voltage-gated Na^+ channels (26). However, even though the charge carried by H^+ influx would be sufficient to induce action potentials, we cannot exclude the possibility that, under physiological conditions, action potentials are evoked synergistically by the current-mediated depolarization and a depolarization that is a consequence of intracellular acidification acting on leak potassium channels (28, 29).

In most sensory cells, transduction currents are carried by Na^+ and Ca^{2+} ions. Na^+ ions are relatively inert and therefore make an ideal charge carrier, whereas Ca^{2+} ions act specifically on a host of Ca^{2+}-binding proteins, tuning the sensory response. Protons are rarely used as charge carriers for electrical signaling in the nervous system, as high concentration of intracellular protons are cell damaging (41). Why, then, would taste cells use a proton channel to mediate sour transduction? Among sensory neurons, the taste cell and the olfactory neuron face a unique problem in that their apical surface is bathed in an extracellular solution that undergoes extreme changes in ionic composition. Olfactory responses of amphibians and fish persist in freshwater because a significant component of the transduction current is carried by outward movement of Cl^- through Ca^{2+}-activated Cl^- channels (42, 43). For sour taste transduction, a proton channel, as opposed to a proton-gated Na^+ channel, would be able to track changes in the concentrations of acids within the oral cavity, without confounding contributions from Na^+ ions, which vary widely in concentration and are detected separately as saltiness.

Materials and Methods

Generation of Transgenic Mice, Immunocytochemistry, and Single-Cell PCR. Generation and validation of transgenic mice is described in *SI Materials and Methods*.

Acute Dissociation of Taste Receptor Cells and Patch-Clamp Recording. Preparation of mouse taste cells and patch clamp recording were previously described (23).For whole-cell recording, the standard internal solution contained the following (in mM): 120 CsAsp, 7 CsCl, 8 NaCl, 5 EGTA, 2.4 $CaCl_2$ (100 nM free Ca^{2+}), 2 MgATP, 0.3 Tris-GTP, and 10 Hepes, pH7.4; the standard bath solution was Tyrode's solution. More information can be found in *SI Materials and Methods*.

Flash Photolysis, Ca^{2+}, and pH Imaging. Flash photolysis and Ca^{2+} imaging were performed as previously described (23). More information is provided in *SI Materials and Methods*.

Suction Electrode Recording. To measure receptor currents, the apical surface of a dissociated taste cell was drawn into a fire-polished pipette with a resistance of 0.5–1 MΩ (~3-μm diameter). The pipette contained 2 mM NPE-caged proton (Tocris) in either Na^+ solution (in mM: 145 NaCl, 5 KCl, 1 $MgCl_2$, 2 $CaCl_2$, 20 dextrose, and 0.1 Hepes, pH 7.4) or Na^+-free solution (in mM: 165 NMDG-Cl, 0.04 $CaCl_2$, and 0.1 Hepes, pH 7.4). Other solutions are described in *SI Materials and Methods*. The apical region was identified as a tapered process that extended from the cell body (Fig. 1*C*). Cells used in this study had similar or more elongated processes than the cell shown Fig. 1*C*. The seal resistance was typically ~5–10 MΩ. Liquid junction potentials were zeroed in the bath before contact with the cell. Records were sampled at 5 kHz and filtered at 1 kHz. When measuring the frequency of action potentials evoked by the UV stimulus, only the cells that fired spontaneous APs were included in the analysis.

ACKNOWLEDGMENTS. We thank N. Segil for technical help in generating transgenic mice, H. Matsunami (Duke University Medical Center, Durham, NC) for anti-PKD2L1 antiserum, D. Liu for help in performing single-cell PCR, and D. Arnold and Y. Wang for careful reading of the manuscript. This work was supported by National Institutes of Health Grant DC004564 (to E.R.L.).

1. Yarmolinsky DA, Zuker CS, Ryba NJ (2009) Common sense about taste: From mammals to insects. *Cell* 139:234–244.
2. Chandrashekar J, et al. (2010) The cells and peripheral representation of sodium taste in mice. *Nature* 464:297–301.
3. Huang AL, et al. (2006) The cells and logic for mammalian sour taste detection. *Nature* 442:934–938.
4. Taylor NW (1928) Acid penetration into living tissues. *J Gen Physiol* 11:207–219.
5. Lyall V, et al. (2001) Decrease in rat taste receptor cell intracellular pH is the proximate stimulus in sour taste transduction. *Am J Physiol Cell Physiol* 281:C1005–C1013.
6. Huang YA, Maruyama Y, Stimac R, Roper SD (2008) Presynaptic (Type III) cells in mouse taste buds sense sour (acid) taste. *J Physiol* 586:2903–2912.
7. Chandrashekar J, et al. (2009) The taste of carbonation. *Science* 326:443–445.
8. Gilbertson TA, Roper SD, Kinnamon SC (1993) Proton currents through amiloride-sensitive Na+ channels in isolated hamster taste cells: Enhancement by vasopressin and cAMP. *Neuron* 10:931–942.
9. Ugawa S, et al. (1998) Receptor that leaves a sour taste in the mouth. *Nature* 395: 555–556.
10. Stevens DR, et al. (2001) Hyperpolarization-activated channels HCN1 and HCN4 mediate responses to sour stimuli. *Nature* 413:631–635.
11. Liu L, Simon SA (2001) Acidic stimuli activates two distinct pathways in taste receptor cells from rat fungiform papillae. *Brain Res* 923:58–70.
12. Lin W, Ogura T, Kinnamon SC (2002) Acid-activated cation currents in rat vallate taste receptor cells. *J Neurophysiol* 88:133–141.
13. Lopez Jimenez ND, et al. (2006) Two members of the TRPP family of ion channels, Pkd1l3 and Pkd2l1, are co-expressed in a subset of taste receptor cells. *J Neurochem* 98:68–77.
14. Ishimaru Y, et al. (2006) Transient receptor potential family members PKD1L3 and PKD2L1 form a candidate sour taste receptor. *Proc Natl Acad Sci USA* 103:12569–12574.
15. Kataoka S, et al. (2008) The candidate sour taste receptor, PKD2L1, is expressed by type III taste cells in the mouse. *Chem Senses* 33:243–254.
16. Richter TA, Dvoryanchikov GA, Roper SD, Chaudhari N (2004) Acid-sensing ion channel-2 is not necessary for sour taste in mice. *J Neurosci* 24:4088–4091.
17. Inada H, et al. (2008) Off-response property of an acid-activated cation channel complex PKD1L3-PKD2L1. *EMBO Rep* 9:690–697.
18. Ishii S, et al. (2009) Acetic acid activates PKD1L3-PKD2L1 channel—a candidate sour taste receptor. *Biochem Biophys Res Commun* 385:346–350.
19. Nelson TM, et al. (2010) Taste function in mice with a targeted mutation of the pkd1l3 gene. *Chem Senses* 35:565–577.
20. Liu D, Zhang Z, Liman ER (2005) Extracellular acid block and acid-enhanced inactivation of the Ca2+-activated cation channel TRPM5 involve residues in the S3-S4 and S5-S6 extracellular domains. *J Biol Chem* 280:20691–20699.
21. Zhang Y, et al. (2003) Coding of sweet, bitter, and umami tastes: Different receptor cells sharing similar signaling pathways. *Cell* 112:293–301.
22. Clapp TR, Medler KF, Damak S, Margolskee RF, Kinnamon SC (2006) Mouse taste cells with G protein-coupled taste receptors lack voltage-gated calcium channels and SNAP-25. *BMC Biol* 4:7.
23. Zhang Z, Zhao Z, Margolskee R, Liman E (2007) The transduction channel TRPM5 is gated by intracellular calcium in taste cells. *J Neurosci* 27:5777–5786.
24. Gong S, Yang XW, Li C, Heintz N (2002) Highly efficient modification of bacterial artificial chromosomes (BACs) using novel shuttle vectors containing the R6Kgamma origin of replication. *Genome Res* 12:1992–1998.
25. DeFazio RA, et al. (2006) Separate populations of receptor cells and presynaptic cells in mouse taste buds. *J Neurosci* 26:3971–3980.
26. Medler KF, Margolskee RF, Kinnamon SC (2003) Electrophysiological characterization of voltage-gated currents in defined taste cell types of mice. *J Neurosci* 23:2608–2617.
27. Yoshida R, et al. (2009) Discrimination of taste qualities among mouse fungiform taste bud cells. *J Physiol* 587:4425–4439.
28. Lin W, Burks CA, Hansen DR, Kinnamon SC, Gilbertson TA (2004) Taste receptor cells express pH-sensitive leak K+ channels. *J Neurophysiol* 92:2909–2919.
29. Richter TA, Dvoryanchikov GA, Chaudhari N, Roper SD (2004) Acid-sensitive two-pore domain potassium (K2P) channels in mouse taste buds. *J Neurophysiol* 92:1928–1936.
30. Gilbertson TA, Avenet P, Kinnamon SC, Roper SD (1992) Proton currents through amiloride-sensitive Na channels in hamster taste cells. Role in acid transduction. *J Gen Physiol* 100:803–824.
31. Decoursey TE (2003) Voltage-gated proton channels and other proton transfer pathways. *Physiol Rev* 83:475–579.
32. Sasaki M, Takagi M, Okamura Y (2006) A voltage sensor-domain protein is a voltage-gated proton channel. *Science* 312:589–592.
33. Ramsey IS, Moran MM, Chong JA, Clapham DE (2006) A voltage-gated proton-selective channel lacking the pore domain. *Nature* 440:1213–1216.
34. Chaudhari N, Roper SD (2010) The cell biology of taste. *J Cell Biol* 190:285–296.
35. Baylor DA, Lamb TD, Yau KW (1979) Responses of retinal rods to single photons. *J Physiol* 288:613–634.
36. Bhandawat V, Reisert J, Yau KW (2005) Elementary response of olfactory receptor neurons to odorants. *Science* 308:1931–1934.
37. Richter TA, Caicedo A, Roper SD (2003) Sour taste stimuli evoke Ca2+ and pH responses in mouse taste cells. *J Physiol* 547:475–483.
38. Okada Y, Miyamoto T, Sato T (1993) Contribution of proton transporter to acid-induced receptor potential in frog taste cells. *Comp Biochem Physiol Comp Physiol* 105:725–728.
39. Lyall V, et al. (2002) Excitation and adaptation in the detection of hydrogen ions by taste receptor cells: A role for cAMP and Ca(2+). *J Neurophysiol* 87:399–408.
40. Ishimaru Y, et al. (2010) Interaction between PKD1L3 and PKD2L1 through their transmembrane domains is required for localization of PKD2L1 at taste pores in taste cells of circumvallate and foliate papillae. *FASEB J* 24:4058–4067.
41. Matsuyama S, Llopis J, Deveraux QL, Tsien RY, Reed JC (2000) Changes in intramitochondrial and cytosolic pH: Early events that modulate caspase activation during apoptosis. *Nat Cell Biol* 2:318–325.
42. Kurahashi T, Yau KW (1993) Co-existence of cationic and chloride components in odorant-induced current of vertebrate olfactory receptor cells. *Nature* 363:71–74.
43. Kleene SJ (1993) Origin of the chloride current in olfactory transduction. *Neuron* 11: 123–132.

Supporting Information

Chang et al. 10.1073/pnas.1013664107

SI Materials and Methods

Generation of BAC Transgenic PKD2L1-YFP Mice. A BAC clone containing the PKD2L1 gene was modified according to published methods (1). Briefly, the shuttle vector pLD53.5SCA-E-B was engineered to contain the sequences Abox-YFP-Bbox, where Abox and Bbox are sequences from the BAC DNA that allow recombination (Fig. S1*A*). Abox is a 504-bp fragment amplified with primers GAATTCAGGCGCGCCGACGACCTTAGGTTTGAGAGGGG (forward) and CCCACAGTCCTACGGGCGTAGAAAG (reverse) that lies between exon 1 and exon 2. B box is a 535-bp fragment from intron 2, amplified with primers GTTACCGCATGCTGTGAGTAGCCGCTGCCTGTG (forward) and GATTGCTTAATTAATGCTCCAGCTTGCTCACAGC (reverse). Note that primers include restriction sites used for cloning. This strategy targets eYFP to the second exon, and was designed to allow splicing of the first two exons and to retain promoter elements that may be located in the first exon. The shuttle vector was electroporated into host cells harboring BAC clone RP23-297k23 (http://bacpac.chori.org), and clones containing cointegrates were selected on Luria broth (LB) plates containing ampicillin and chloramphenicol (Chl). Colony PCR with oligos specific for Abox, Bbox, and YFP was used to confirm cointegration. Clones containing correctly resolved BACs were further selected on LB/Chl plates and confirmed by colony PCR. DNAs of correctly resolved BACs were purified based on a modification of Quiagen Midi prep kit. Southern blot with DIG probes (Pierce) against Abox, Bbox, and YFP confirmed the correct insertion of YFP without other large-scale modification of the BAC. BAC DNA purified by cesium chloride gradients was used to generate transgenic mice by the University of Southern California (USC) Transgenic Core Facility. Founder mice were identified by PCR and mated with WT mice (B6/D2). Mice were genotyped with two pairs of primers (1): GATGTACTACCCGGGATCCACCGGTCGCC (forward) and GCTCCGCGAGCTCTAGGGCCGCTTTACTTGTAC (reverse; recognizes 650-bp fragment from YFP), and (2) GCTGCTGTCTCCATATCTGTCGG (forward) CGGACACGCTGAACTTGTGGCC (reverse; 700-bp product) using the following program: 94 °C, 5 min followed by 40 cycles of 94 °C, 30 s; 58 °C, 30 s; 72 °C, 45 s; and a final extension at 72 °C for 7 min.

Animals. All experimental procedures were approved by the Institutional Animal Care and Use committee of the University of Southern California. Transgenic mice in which expression of eGFP is driven by TRPM5 promoter (TRPM5-GFP) and mice carrying a targeted deletion of PKD1L3 gene (PKD1L3$^{-/-}$) were described previously (2–5). The latter strain of mice were mated with PKD2L1-YFP mice to generate animals that were positive for YFP and were negative for PKD1L3 expression (PKD2L1-YFP/PKD1L3$^{-/-}$).

Single-Cell RT-PCR. Single-cell RT-PCR analysis was performed using a modification of published methods (6). Briefly, a single GFP (+) or YFP (+) taste receptor cell isolated from CV papillae was transferred into a PCR tube containing the following: 1.5 mM $MgCl_2$, 0.5% Nonidet P-40, 5 mM DTT, 50 μM dNTPs, 200 ng/mL Anchor T primer, 0.4U/μL Rnasin, and 0.3U/μL Prime RNase Inhibitor in 1× PCR buffer. The reaction was incubated at 65 °C for 1 min to denature the RNA and then at 37 °C for 90 min with reverse transcription mix [Superscript II (Invitrogen), 0.5 μL RNase inhibitor]. Tailing was performed at 37 °C, 20 min after the addition of TdT mix containing the following: 1.5 mM $MgCl_2$, 3 mM dATP, 1.25 U/μL TdT, and 0.05 U RNase H in 1× PCR buffer. The product was added to PCR mix [0.25 mM dNTP, 20 ng/mL Anchor T, and 2.5 U Ex Taq HS polymerase (Takara) in 1× Ex Taq Buffer] and subjected to amplification using the following protocol: (95 °C, 2 min; 37 °C, 5 min; 72 °C, 20 min followed by 30 cycles of 95 °C, 30 s; 67 °C, 1 min; 72 °C, 6 min + 6 s/cycle). To determine whether a gene of interest was present in the single-cell cDNA, the single-cell product was diluted 1:1,000 in the final PCR mix containing the following: 0.25 mM dNTP, 0.5 μM of each primer, and 0.25 U Taq polymerase in 1× Taq Buffer. The PCR protocol was as follows: 95 °C, 10 min followed by 30 cycles of 95 °C, 15 s; 55 °C, 30 s; and 72 °C, 1 min. TRPM5 was detected with CCAGGTGGTGCAAGGC (forward) and CCTCAGCACCTCCCCC (reverse). PKD2L1 was detected with GGGCAGGCTCACAAGC (forward) and GGTAGCGAAGCCGATGC (reverse). SNAP-25 was detected with CGTGTGGTGGATGAACGG (forward) and GGAGAGCACAGCAGAAGG (reverse).

Immunohistochemistry. Sectioning and staining of frozen tissue sections were as described previously (4). Sections were incubated with anti-GFP antibody (1/1,000; Invitrogen), anti-PKD2L1 antiserum (1/1,000 dilution) (7), or anti-TRPM5 antiserum (1/500 dilution) (4). All antibodies were previously validated to label the specific populations of taste cells against which they were directed (4, 7). Secondary antibodies conjugated to Alexa-488 or Alexa-594 (Invitrogen) were used at a 1/500 dilution. Images were acquired with a Zeiss 510 Meta confocal microscope.

Acute Dissociation of Taste Receptor Cells. In brief, lingual epithelium was peeled from the tongue by injecting a solution containing 1 mg/mL elastase (Worthington) and 2.5 mg/mL dispase II (Roche) dissolved in Tyrode's solution (in mM: 145 NaCl, 5 KCl, 1 $MgCl_2$, 2 $CaCl_2$, 20 dextrose, and 10 Hepes, pH 7.4) between the epithelium and the muscle layer, and incubating the intact tissue for 20 min at room temperature in a large volume of bath solution containing either Tyrode's solution (standard) or Ca^{2+}-free saline (for non-enzymatically prepared cells; in mM: 150 NaCl, 0.5 EGTA, and 10 Hepes, pH 7.4), bubbled with 95% O_2/5% CO_2 (4, 8–10). A small piece of the epithelium containing circumvallate papillae was further incubated in the enzyme mixture for 20 min at room temperature. The reaction was stopped by washing the tissue in Ca^{2+}-free saline. For some experiments, enzymes were used only to peel the epithelium, and taste buds were isolated from the peeled epithelium following incubation in Ca^{2+}-free saline for 10–20 min by gentle suction into a fire-polished micropipette. This preparation was considered nonenzymatic, as enzyme access to the apical surface of the cell was limited. For both preparations, single cells were isolated by trituration in Tyrode's solution and were used within 6 h.

Patch-Clamp Recording. Patch-clamp recording was performed as previously described (4). Extracellular solution in most cases was exchanged by moving a linear array of microperfusion pipes (Warner Instruments). For most whole-cell recordings, membrane potential was held at −80 mV and ramped from −80 mV to +80 mV (1 V/s). Significance was determined by a two-tailed Student *t* test.

Transfection of HEK 293 Cells. PKD2L1 and HA-tagged PKD1L3 (at 10:10:1 with GFP) (7) or rat TRPV1 (at 20:1 with GFP) were transiently transfected into HEK-293 cells using TransIT-LT1 Transfection Reagent (Mirus Bio Corporation). Recordings from

GFP-positive cells were performed ~24–48 h after transfection at room temperature.

Solutions. For whole-cell recording, acid solutions contained the following (in mM): 150 NaCl, 2 $CaCl_2$, buffered either with Mes (10 mM, pH 5 or 6) or with acetic acid (HOAc, 10 mM, pH 6, and 2 mM, pH 5, or 20 mM, pH 4). K^+ internal solution contained the following (in mM): 120 KAsp, 20 KCl, 10 Hepes, 2 MgATP, 0.3 GTP, and 3 Na_2ATP, pH7.4. To measure ionic selectivity, extracellular Na^+ was replaced with 150 mM TEA^+ or 165 mM $NMDG^+$. For high Cl^- internal solution, 120 mM Asp^- was replaced by 120 mM Cl^-. Acid solutions containing 150 mM TEA^+ were adjusted to different pHs (4.5, 5, 5.5, or 6) with 10 mM Mes. The following chemicals were added to the pH 5 solution (in mM): 1 $CdCl_2$; 0.1 desipramine; 200 nM Bafilomycin A1; 1 $ZnCl_2$; and 30 μM amiloride. For loose patch recording, bath solution and pipette solution contained the following (in mM): 150 NaCl, 2 $CaCl_2$, and 10 Hepes, pH7.4. NaCl, 25 mM, was replaced with KCl, 25 mM, for K^+ stimulation. For experiments characterizing voltage-gated Ca^{2+} channels in PKD2L1-expressing taste cells, the internal solution contained the following (in mM): 120 CsAsp, 20 CsCl, 2 MgATP, 10 Hepes, 20 EGTA, pH7.4, and bath solution contained 125 $NMDG^+$, 20 $BaCl_2$, and 10 Hepes, pH 7.4. High K^+ stimulus solution contained (in mM) 150 KCl, 2$CaCl_2$, and 10 Hepes, pH 7.4.

Flash Photolysis, Ca^{2+}, and pH Imaging. Flash photolysis and Ca^{2+} imaging were performed as previously described (4). In brief, cells were illuminated with UV light from a mercury arc lamp that was passed through a ×350/50 band pass filter (Chroma Technology) controlled by a Uniblitz shutter (Vincent Associates). The shutter was opened for 500 ms to uncage H^+. For experiments in which changes in intracellular Ca^{2+} levels were measured, cells were loaded with fura-2 AM, and fluorescence emission was measured in response to excitation from a xenon arc lamp at 340 nM (300 ms) and 380 nM (36 ms). Uncaging was achieved by manually opening the 380xv1 band pass filter for ~2–3 s. To minimize uncaging during image acquisition, the illumination field was reduced to include only the cell under study. To measure changes in intracellular pH, cells were loaded with a pH-sensitive fluorescent dye Oregon Green 488 carboxylic acid diacetate (carboxy-DFFDA; Invitrogen) according to the manufacturer's instructions. The fluorescence emission was detected using a GFP filter set (Olympus).

Chemicals. Acetic acid and amiloride were purchased from EMD biosciences. Fura-2 AM and Oregon Green 488 carboxylic acid diacetate were purchased from Invitrogen Molecular Probes. Other chemicals including HCl, propionic acid, $ZnCl_2$, DIDS, DCCD, Bafilomycin A1, desipramine, and NPPB were all purchased from Sigma.

1. Gong S, Yang XW, Li C, Heintz N (2002) Highly efficient modification of bacterial artificial chromosomes (BACs) using novel shuttle vectors containing the R6Kgamma origin of replication. *Genome Res* 12:1992–1998.
2. Clapp TR, Medler KF, Damak S, Margolskee RF, Kinnamon SC (2006) Mouse taste cells with G protein-coupled taste receptors lack voltage-gated calcium channels and SNAP-25. *BMC Biol* 4:7.
3. Damak S, et al. (2006) Trpm5 null mice respond to bitter, sweet, and umami compounds. *Chem Senses* 31:253–264.
4. Zhang Z, Zhao Z, Margolskee R, Liman E (2007) The transduction channel TRPM5 is gated by intracellular calcium in taste cells. *J Neurosci* 27:5777–5786.
5. Nelson TM, et al. (2010) Taste function in mice with a targeted mutation of the pkd1l3 gene. *Chem Senses* 35:565–577.
6. Mizrahi A, Matsunami H, Katz LC (2004) An imaging-based approach to identify ligands for olfactory receptors. *Neuropharmacology* 47:661–668.
7. Ishimaru Y, et al. (2006) Transient receptor potential family members PKD1L3 and PKD2L1 form a candidate sour taste receptor. *Proc Natl Acad Sci USA* 103:12569–12574.
8. Spielman AI, et al. (1989) A method for isolating and patch-clamping single mammalian taste receptor cells. *Brain Res* 503:326–329.
9. Béhé P, DeSimone JA, Avenet P, Lindemann B (1990) Membrane currents in taste cells of the rat fungiform papilla. Evidence for two types of Ca currents and inhibition of K currents by saccharin. *J Gen Physiol* 96:1061–1084.
10. Huang YA, Maruyama Y, Stimac R, Roper SD (2008) Presynaptic (Type III) cells in mouse taste buds sense sour (acid) taste. *J Physiol* 586:2903–2912.

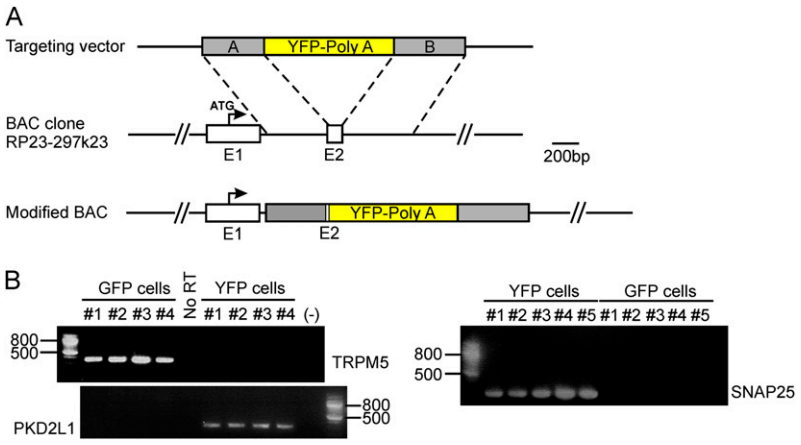

Fig. S1. Generation of PKD2L1-YFP BAC transgenic mice. (*A*) Modifed BAC clone used to generate transgenic mice. YFP was inserted in frame in the second exon of PKD2L1. (*B*) RT-PCR analysis of mRNAs isolated from single YFP-positive taste cells dissociated from PKD2L1-YFP mice or single GFP-positive taste cells dissociated from TRPM5-GFP mice. Each lane represents a single cell. Expression of PKD2L1 (*Lower Left*) as well as SNAP-25 (*Right*) is observed in YFP-positive but not GFP-positive cells, whereas TRPM5 (*Upper Left*) was detected in GFP-positive and not YFP-positive cells.

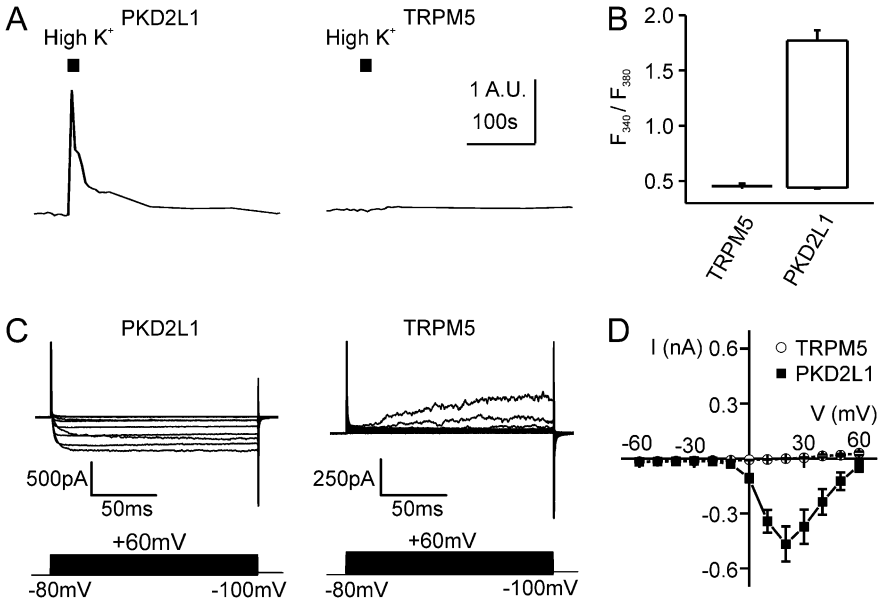

Fig. S2. Expression of voltage-gated Ca^{2+} channels in PKD2L1-YFP taste cells. (*A*) Ca^{2+} elevation in response to KCl depolarization (150 mM KCl), an indicator of the expression of voltage-gated Ca^{2+} channels (1), was observed in PKD2L1-YFP cells (*Left*) and not in TRPM5-GFP cells (*Right*) (*B*) Average data from experiments as in *A*. Bottom of the bar represents the average F_{340}/F_{380} ratio before KCl stimulus. Height of the bar represents the peak ratio after KCl stimulus. (*C*) Currents recorded with 20 mM Ba^{2+} (125 mM $NMDG^{+}$) in the bath from a PKD2L1-YFP cell (*Left*) and a TRPM5-GFP cell (*Right*) in response to voltage steps from −100 mV to +60 mV. Only the YFP cell exhibited inward Ba^{2+} currents, carried by voltage-gated Ca^{2+} channels. (*D*) Average I-V data from experiments as in (*C*). Data represent mean ± SEM.

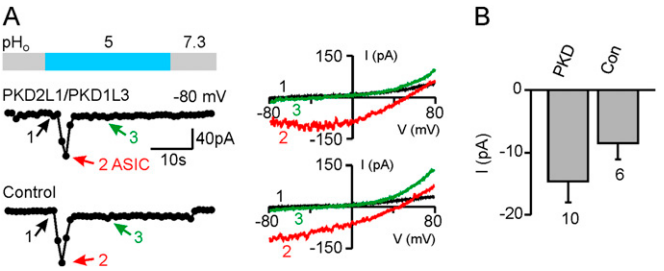

Fig. S3. PKD1L3/PKD2L1 channels are not activated by pH 5 HCl. (*A*) Responses of HEK 293 cells coexpressing PKD1L3/PKD2L1 and of untransfected HEK 293 cells to pH 5 (HCl). A rapidly inactivating ASIC current was activated in both transfected and control cells. I-V curve measured at the time points indicated are shown at *Right*. (*B*) Average current at −80 mV from experiments as in *A*, measured 15 s after stimulus delivery (green trace in *A*). Data represent mean ± SEM. No significant difference was observed between groups ($P = 0.21$).

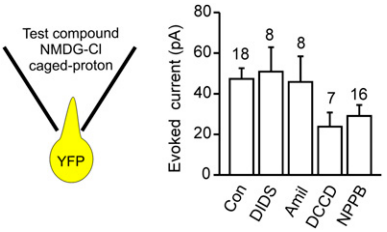

Fig. S4. Pharmacology of the responses to apical delivery of protons in PKD2L1-YFP taste cells. Effect of potential blockers was assessed by measuring responses to uncaging of NPE-caged proton with suction electrode in the presence and absence of the chemical (Fig. 4C). The following chemicals and quantities were tested: 200 μM DIDS, 100 μM Amiloride, 200 μM DCCD, and 100 μM NPPB. The pipette solution was Na^{+} free. Data represent the peak response (mean ± SEM). For none of the drugs tested was the magnitude of the response in the presence of the drug significantly different from the magnitude of the control response ($P > 0.05$ for all comparisons).